Environmental Science
Water Research & Technology

ROYAL SOCIETY OF CHEMISTRY

PAPER

View Article Online
View Journal

Cite this: DOI: 10.1039/c9ew00915a

Stable immobilized amine sorbents for heavy metal and REE removal from industrial wastewaters†

Walter Christopher Wilfong, *[ab] Brian W. Kail,[ab] Qiuming Wang,[ac] Fan Shi,[ab] Greg Shipley,[d] Thomas J. Tarka[a] and McMahan L. Gray*[a]

Received 15th October 2019,
Accepted 24th March 2020

DOI: 10.1039/c9ew00915a

rsc.li/es-water

Pollution of precious water systems with heavy metals predicates the need to eliminate them from industrial process or mining effluents prior to discharge to sustain this vital resource. Herein, we developed H_2O-stable basic immobilized amine sorbents (BIAS) from a combination of *N*,*N*-diglycidyl-4-glycidyloxyaniline tri-epoxide crosslinker (E3) and polyethylenimine (PEI). Stability screening was accomplished through thermal gravimetric analysis decompositions and CO_2 capture studies. Amine leach resistance of the optimized formula, PES-0.43-500 (40 wt% E3/PEI-0.43 on 500 μm SiO_2) was further analyzed by CHNS analysis and diffuse reflectance infrared Fourier transform spectroscopy (DRIFTS). Examination of wash solution with our UV-vis/Cu^{2+} amine quantification technique confirmed TGA results. Sequential impregnation of SiO_2 with E3/PEI was monitored *in situ* by DRIFTS and distinguished an interfacial, hydrogen-bonded E3–PEI···SiO_2 layer from a bulk crosslinked E3–PEI network. Comparative adsorption tests were conducted with PES-0.43-500, S930PLUS cation exchange resin, and pine biochar for toxic (Pb, Cd, Hg, Se, Ar, Se), valuable (La through Yb REE's), and other heavy (Al, Mn, Zn, Cu, *etc.*) metals removal/recovery from synthetic and real solutions. High affinity of PES-0.43-500 towards Cr, As, and Se and its high Hg (99.2%) and Pb (98.2%) uptakes from a six-element mixture translated well to commercial flue gas desulfurization water discharge (FGD, pH 6.7) and Pb-spiked tap water. Near-complete recovery of all REE's from local acid mine drainage (AMD-PBG, pH 3.6) outperformed the resin and was closely mirrored during 5-cycle REE recover-strip testing with synthetic AMD (pH 2.6). Robust performance and easy scalability of green BIAS materials make them attractive for commercialization.

Water impact

Novel, stable immobilized amine sorbents uniquely removed/recovered cationic and oxyanionic toxic heavy metals plus valuable rare earth elements from commercial flue gas desulfurization discharge and acid mine drainage waters.

Introduction

Widespread contamination of Earth's water systems with a myriad of heavy metals continues to grow and become an increasing threat to our way of life.[1–5] Most notably for the heavy metals, the U.S. Resource Conservation and Recovery Act (RCRA) classified arsenic, cadmium, chromium, lead, mercury and selenium in cationic or anionic form as posing a significant health risk due to their toxicity.[6] Besides these RCRA metals, Cu is also regulated by the EPA particularly for drinking water (lead and copper rule)[7] while the toxicity criteria for Al regarding freshwater aquatic life has been updated to improve the ecosystem.[8] Remediation of these plus a variety of other metals, especially at the contamination source, is urgently needed to ensure the sustainability of our precious clean water resources and infrastructures.

Contributing sources for heavy metal contaminants found in potable water, rivers, ground water, and other bodies include runoff from electronics and steel production, corrosion of household plumbing, hydraulic fracturing, acid

[a] National Energy Technology Laboratory, 626 Cochrans Mill Road, P.O. Box 10940, Pittsburgh, PA 15236-09040, USA. E-mail: walter.wilfong@netl.doe.gov
[b] Leidos Research Support Team (LRST), 626 Cochrans Mill Road, P.O. Box 10940, Pittsburgh, PA 15236-09040, USA
[c] Oak Ridge Institute for Science and Education (ORISE), P.O. Box 117, Oak Ridge, TN 37831, USA
[d] BioEnergy Development, 4004 Stags Leap Way, Paso Robles, CA 93446, USA

† Electronic supplementary information (ESI) available: Solution metal concentrations; test procedure for solution analysis; DRIFTS spectra of PES-*X*-100 sorbents and PES-0.43-500 with adsorbed metals; treatment of single-element RCRA solutions with PES-0.43-500; SEM of fresh and spent sorbent; treatment of AMD-PBG with activated carbon; kinetic metal uptake profiles. See DOI: 10.1039/c9ew00915a

mine drainage (AMD) discharged from active or abandoned metal and coal mines, plus others.[9–11] Beyond acid mine drainage, other coal wastewater sources like those derived from coal-fired power plant ash ponds or ash dumps and flue gas desulfurization (FGD) effluents contain high concentrations of heavy metals. Field samples of FGD, AMD, and ash pond or dump leachate were found to contain low ppb to high ppm concentrations of RCRA species; Ni, Zn, V, B, Fe, Cu, Al, Be, Co, Li, Mo, Mn, Tl, Sr; and others (not all present in every water type).[11–13]

Accompanying the toxic metals in coal waste waters, primarily acid mine drainage, are valuable rare earth elements. Only 1.3% of the global reserves are controlled by the United States while 59% are controlled by Brazil and China.[14] The U.S.'s limited REE supply presents a national security risk, motivating research conducted by the US Department of Energy and other institutions for recovering REE's from domestic sources, including water.[15–18] Recovery of aqueous REE's from AMD is a green method alternative to that of mining and processing the solid REE's. The mining/processing activities deteriorate the surrounding environment and generate greenhouse gas emissions on the order of 2430 GJ CO_2 per tonne REE oxide.[19,20]

Among the most common methods for extracting the toxic and valuable heavy metals from different water sources, liquid–liquid extraction; membrane separation; and adsorption; the latter is most attractive because it facilitates both fast uptake of the aqueous metals and easy separation of the treated solution from the solid sorbent. Polymeric ion exchange resins (IER),[21,22] zeolites,[23] and activated carbons plus biochars[24,25] are well studied sorbents because of their proven performance and long-standing utilization in household and industrial applications. Amberlite (DuPont), Advera (PQ Corporation), and Centaur (Calgon) brands are typical examples of these materials. Lesser known due to lack of commercialization are functionalized silica sorbents. These contain grafted, as-is (3-aminpropyl)triethoxysilane (APTES)[26] and ligand-modified furan-2,4-diamido-propyltriethoxysilane/APTES and diethylenetriaminepenta-acetic dianhydride/APTES aminosilanes;[19,27] ligand-modified ethylenediaminetetraacetic acid/chitosan–silica hybrids;[28] and impregnated aminoacids (L-cysteine) or polyamines (polyethylenimine).[29]

H_2O-Stable grafted sorbents sometimes afford relatively limited metal uptake by their monolayer of coverage, whereas the unstable/leachable amines comprising the bulk layers of impregnated sorbents introduce a secondary source of contamination. Although activated carbon and biochar are ubiquitously available for/as water treatment systems, their high processing/activating temperatures (300–900 °C) can generate a relatively high carbon footprint compared to that of typical silica supports used for the amine-functionalized sorbents. Some life cycle assessments estimated that the Global Warming Potential for activated carbon (AC) and biochar (BC) can be between 4.7 (calculated from data table) and 9.3 kg CO_2-eq. per kg AC, BC (no CO_2 capture) compared to 4.1 for a typical precipitated silica.[30–32]

Herein, we developed novel crosslinked epoxy–amine, *N*,*N*-diglycidyl-4-glycidyloxyaniline (E3)–polyethylenimine/silica sorbents for extraction of toxic heavy metals and REEs from synthetic and real solutions. An array of materials was prepared by simple wet impregnation, then screened for H_2O stability by water washing and for availability of amine sites by CO_2 capture. Retention of >91% impregnated E3–PEI species after prewashing the optimized sorbent, PES-0.43-500, was attributed to amine–epoxy crosslinking (DRIFTS) and confirmed by analyzing the aqueous amine content with a UV-vis/Cu^{2+} technique. Metal extraction from synthetic solution revealed high affinity towards oxyanionic Cr(VI) (92.8%), As(V) (65.6%), and Se(VI) (47.0%) compared to a commercial cation exchange resin and biochar. Uptakes of Cd^{2+}, Pb^{2+}, and Hg^{2+} mixed with the oxyanions were similar for all sorbents. The extraction trends for Cr, Pb, and Hg were similarly observed for industrial FGD water, where the sorbent further showed good affinity for Re, Zn, Ni, and Mn. Cyclic adsorption–desorption of ~90% REE's from a synthetic AMD solution, and successful removal of >90% of Pb from spiked tap water to below US Environmental Protection Agency (EPA) limits further proved the efficacy of this sorbent for real applications.

Experimental

Materials and reagents

Polyethylenimine, branched with molecular weight 800 g mol^{-1} (PEI_{800}, $H_2O \leq 2\%$, Sigma-Aldrich), *N*,*N*-diglycidyl-4-glycidyloxyaniline (E3, 95–106 g mol^{-1} epoxide equivalent, purity ≥90.0%, Sigma-Aldrich), and amorphous silica (PQ Corporation, type CS-2129) with 100 and 500 μm avg. particle sizes comprised the immobilized amine sorbent. Methanol (ACS, Fisher Scientific) served as a solvent for sorbent preparation. Commercial samples of PUROLITE S930 PLUS cation exchange resin and pine biochar sorbents were provided by Purolite and BioEnergy Development, respectively.

A 500 ppm $CuCl_2$ (97%, Sigma Aldrich)/ultrapure water (Milli-Q) solution was used to quantify aqueous amine concentrations in wash solutions. The following additional species were used to prepare single- or mixed-element REE and heavy metal solutions: REE's – $LaCl_3$ (anhydrous, 99.9% trace metals basis), $NdCl_3{\cdot}6H_2O$ (99.9% trace metals basis), $EuCl_3{\cdot}6H_2O$ (99.9% trace metals basis), $DyCl_3{\cdot}6H_2O$ (≥99.99% trace metals basis), $YbCl_3{\cdot}6H_2O$ (99.9% trace metals basis); alkali/alkaline – Na_2SO_4 (anhydrous, ACS), $MgCl_2{\cdot}6H_2O$ (ACS), $CaCl_2$ (anhydrous); heavy metal cations – $PbCl_2$ (98%), $CdCl_2$ (tech. grade), $HgCl_2$ (ACS reagent, ≥99.5%), $MnSO_4{\cdot}H_2O$ (99+%, extra pure), $Al_2(SO_4)_2{\cdot}18H_2O$ (98+% ACS), $Fe_2(SO_4)_3{\cdot}5H_2O$ (97%); heavy metal oxyanions – Na_2CrO_4 (98%), $Na_2HAsO_4{\cdot}7H_2O$ (≥98.0%), Na_2SeO_4 (>95%). Commercial field samples of flue gas desulfurization water derived from coal combustion and acid mine drainage runoff were provided by AquaTech and a local botanical garden,

respectively. Tap water was taken from the lab faucet and spiked with 125 ppb of Pb.

Sorbent preparation

An array of immobilized amine sorbents, each having 50 wt% organic loadings, was prepared by our previously-reported procedure. Several 2.0 to 5.0 g portions of PEI_{800} and 0.0 to 3.0 g of E3 were dissolved in 100.0 g MeOH at E3/PEI_{800} ratios from 0.13/1 to 1.5/1. Each of the resulting impregnation solutions was mixed with 5.0 g of 100 μm SiO_2 in a 250 mL round-bottom flask set inside of a rotary-evaporator maintained at 40 °C and 100 rpm. MeOH was gradually evaporated from the solid/liquid mixture by step-wise reducing the initial 760 mmHg system pressure to 360 mm Hg for 30 min; 110 mmHg for 20 min; then 20 mmHg for 10 min. After 1 hour of drying under vacuum, atmospheric pressure was restored and the sample moved to a 105 °C oven for 30–60 min for final drying and completion of the amine–epoxy reaction. The sorbent was impregnated and dried at a relatively low temperature, 40–55 °C, to minimize premature E3–PEI crosslinking outside the SiO_2 pores.

An array of similar 500 μm sorbents was prepared at a 40 wt% organic loading and with the same E3/PEI_{800} ratios. Larger particle size is expected to facilitate better flow of metal solution through the packed sorbent bed. Sorbents were labelled with the scheme, "PES-*X*-*Y*", where "PES" denotes the base formula "PEI–epoxy–silica", *X* represents the E3/PEI_{800} ratio, and *Y* represents the particle size of 100 or 500 microns.

Water stability testing

All immobilized amine sorbents were tested for their H_2O stability using our previously published accelerated water washing method.[33] Here, 0.5 g beds of sorbent were set atop a ceramic frit inside a 1.0 cm-diameter glass column (4.0 mL) and exposed to 20 mL of 0.5 mL min^{-1} flowing ultrapure water. Organic content of the fresh and washed sorbents was ascertained through thermal gravimetric analysis (TGA, Q500, TA Instruments) decomposition studies and CO_2 adsorption tests. Thermal decompositions were performed in the TGA by first pretreating the sorbents at 105 °C in 60 mL min^{-1} flowing N_2 for 90 min to remove H_2O and CO_2 preadsorbed from the environment; ramping at 20 °C min^{-1} up to 800 °C in a 60 mL min^{-1} air flow and holding for 30 min; then cooling down. Sorbent organic content retained (OCR) values after washing were calculated as, OCR = wt% $Organic_{washed}$/wt% $Organic_{fresh}$ × 100%.

CO_2 adsorption runs were accomplished in the TGA on similarly pretreated sorbents. A 14% CO_2/N_2 flow was passed through the reactor cell at 75 °C for 30 min, causing a weight increase in the sorbent that was used to calculate CO_2 capture capacity (mmol CO_2 per g-sorb.). Percentage of CO_2 capture retained (PCR) values were calculated as, CO_2 $ads._{washed}/CO_2$ $ads._{fresh}$ × 100%. Higher OCR and PCR values directly reflected sorbents more stable towards organics leaching during water treatment.

Metal uptake evaluation

Six total solutions, whose exact compositions can be found in Table S1 in the ESI,† were tested in the flow column: (i) 5 REE – ~50 ppm each of La^{3+}, Nd^{3+}, Eu^{3+}, Dy^{3+}, Yb^{3+} (250 ppm total) REE's at pH 5.3 ± 0.05; (ii) RCRA – ~25 ppm each of Pb^{2+}, Cd^{2+}, Hg^{2+}, Se^{6+}, Cr^{6+}, As^{5+} (150 ppm total) heavy metals at pH 6.2; (iii) AMD-SYN – synthetic acid mine drainage at pH 2.6; (iv) FGD – commercial flue gas desulfurization water discharge at pH 6.7; (v) AMD-PBG – local acid mine drainage runoff at pH 3.6; and (vi) Pb-spiked tap – ~125 ppb Pb-spiked tap water at pH 5.7. Because solution (ii) was somewhat unstable and formed precipitates while aging, uptake tests were completed within 1 hour of its preparation.

Room-temperature metal removal/recovery tests were first performed on washed sorbents either in flow or batch configuration. Adsorption under flowing conditions was conducted in a separate glass column identical to that used for sorbent washing. A 0.5 g sample of immobilized amine sorbent (washed), pine biochar (425–600 μm, washed), or as-is S930PLUS (425 to 1000 μm) cation exchange resin was loaded into the column and 20 mL of 0.5 mL min^{-1} flowing aqueous metal solution was passed over the sorbent bed *via* a peristaltic pump. Treated solution exiting the column was collected in a 50 mL polystyrene vial and submitted along with fresh stock solution for inductively coupled plasma mass spectrometry (ICP-MS), optical emission spectroscopy (OES), and cold vapor atomic absorption spectroscopy (CVAAS, for Hg) analyses of aqueous metal concentrations (see ESI† for analysis procedures). To ensure the validity of all data per the analytical procedure, metal concentrations in the treated solutions below the reporting limit were taken at that limit and used for metal uptake calculations.

A 5-cycle, recover-strip test was performed with AMD-SYN as the contaminant solution and pH 8.5 ammonium citrate–ammonium hydroxide buffer as the stripping agent. A 20 mL volume of AMD-SYN was first passed over the 0.5 g sorbent bed at 0.5 mL min^{-1}, followed by the same volume of ammonium citrate/ammonium hydroxide buffer solution; this completed one cycle. A total of 5 cycles was performed. A 1 min air purge of the column and lines after each individual AMD-SYN and buffer step ensured removal of remaining interstitial solution trapped between the particles.

Relative maximum metal uptake tests were conducted for each sorbent type in batch mode by soaking 0.150 g samples in 50 mL of separate 5 mM Eu^{3+} (pH = 5.0), Cd^{2+} (pH = 5.1), or Cr^{6+} (pH = 7.7) solutions for 17–24 hours. Following metal uptake, the treated solutions were decanted from the sorbents and analyzed for aqueous metal content.

Sorbent characterization

Brunauer–Emmett–Teller (BET) surface areas and Barrett–Joyner–Halenda (BJH) pore volumes plus pore size

distributions of pretreated washed biochar and SiO_2 (250 °C, 24 hours, vacuum) plus associated immobilized amine sorbents (110 °C, 24 hours, vacuum) were determined by N_2 physisorption measurements at 77 K using a Quantachrome NOVA 2200 surface analyzer.

Carbon–hydrogen–nitrogen–sulfur (CHNS) assessment of the sorbents was carried out with a Perkin Elmer II Series CHNS elemental analyzer to determine the N content of the fresh materials. Generally, solid sorbents were combusted in an oxygen rich environment, where the generated gases were analyzed with a frontal chromatography unit.

Diffuse reflectance infrared Fourier transform spectroscopy (DRIFTS) analysis was performed on the immobilized amine sorbents to assess their chemical structure. About 10–20 mg of sorbent were loaded into the sample cup of a DRIFTS SMART accessory set inside a Nicolet 8700 infrared spectrometer (ThermoScientific). IR single beam spectra of pretreated sorbents (120 °C, N_2, 30 min) were obtained at 50 °C by averaging 25 co-added scans collected over 15 s with a 4 cm^{-1} resolution.

DRIFTS was further utilized to perform *in situ* impregnation of SiO_2 with 40 wt% of E3/PEI_{800}, according to the optimum sorbent formula. About 6–7 mg of ground 500 μm SiO_2 were tightly packed into a metal cup set inside the ceramic DRIFTS sample cup, which was sealed with a dome housing ZnSe windows (4000 to 600 cm^{-1} range). The SiO_2 sample was pretreated at 110 °C under N_2 flow for 60 min then cooled to 40 °C. The temperature of the SiO_2 bed was previously verified by placing a thermocouple on the cup surface and monitoring the temperature during heating and cooling. Subsequently the dome was removed, 16 μL of 7.9 wt% E3/PEI_{800}-0.43 in MeOH were injected onto the surface of the SiO_2 bed, then the dome was replaced. The wet mixture then sat at 40 °C under N_2 flow for 90 min to evaporate nearly all MeOH. Following, the sample was heated at 110 °C for 60 min to evaporate any remaining solvent and to crosslink PEI with E3, then the sample was cooled back down. This deposited about 13 wt% organics on the SiO_2 surface, which was previously equated to a near monolayer of coverage.[34] A second injection of 26.3 wt% E3/PEI was deposited onto SiO_2, followed by MeOH evaporation, crosslinking, and cooling. This deposited about 27 wt% organics on SiO_2 as bulk species to give a 40 wt% total loading.

Results and discussion

Sorbent stability and CO_2 capture screening

Immobilized amine sorbents were prepared by co-impregnating SiO_2 with polyethyleneimine (metal adsorption sites) and *N*,*N*-diglycidyl-4-glycidyloxyaniline, a tri-epoxide that covalently crosslinks PEI. Crosslinking dramatically enhanced the leach resistance of the amine molecules and rendered the sorbent water-stable during aqueous metal extractions. TGA decomposition and CHNS elemental analysis results in Table 1 show that the fresh 100 μm size sorbents contained

Table 1 Immobilized amine sorbent organic and amine content plus CO_2 capture capacity. The wt% N values were determined from CHNS analyses. CO_2 capture amine efficiency (mol CO_2/mol NH_2 + NH) was calculated, in part, from the wt% N. Sorbent PS-0-100 contained no E3

Sorbent	Organic loading (Wt%)	Amine content (Wt% N; mmol N per g-sorb.)	CO_2 capture (mmol CO_2 per g-sorb.; mol CO_2 per mol NH_2 + NH)
PS-0-100	48.3	14.47; 10.34	2.79; 0.4
PES-0.13-100	50	14.34; 10.24	2.06; 0.32
PES-0.20-100	49.6	13.13; 9.38	1.8; 0.3
PES-0.28-100	47.6	12.26; 8.76	1.57; 0.29
PES-0.43-100	44.7	11.06; 7.9	1.22; 0.27
PES-0.67-100	44.2	9.86; 7.04	0.69; 0.18
PES-1.5-100	50.0	7.42; 5.3	0.11; 0.04

44.2 to 50.0 wt% organics. The decreasing mmol N per g-sorb. content with increasing E3/PEI ratio results from substitution of PEI with E3 and reflects diminished adsorptive performance when the sorbents' primary (–NH_2) and secondary (–NH) amines were reduced.

Fig. 1 confirms the loss in active amine sites through low mmol CO_2 per g-sorb. gas capture at higher E3/PEI values, where more primary and secondary amines were converted into tertiary amines through crosslinking. Amine-based sorbents are widely known to adsorb dry CO_2 by –NH_2 and –NH groups, excluding –N groups, as ammonium–carbamate ion pairs and carbamic acid.[35,36] Therefore, CO_2 may serve as a probe molecule to estimate the availability of –NH_2 and –NH sites for metal adsorption. Here, we use the trend in sorbent CO_2 capture capacity to screen for their metal adsorption potentials. Sharp exponential growth in the PCR and OCR values inversely mirrors the exponential decay in CO_2 capture capacity up to a critical E3/PEI weight ratio of X = 0.43; a –CH–O–CH_2–(epoxy)/–NH_2, –NH molar ratio of 0.32. This indicates the formation of an extensive, crosslinked

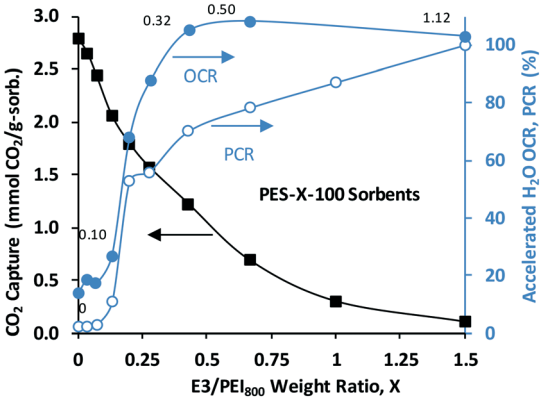

Fig. 1 CO_2 capture performance plus PCR and OCR values for 100 μm-size immobilized amine sorbents. OCR and PCR values represent amine leach resistance/sorbent water stability. Numbers beside the OCR profile represent the epoxy/amine (primary plus secondary amines) group molar ratio.

PEI–E3–PEI network that joins separate PEI molecules within the SiO_2 pores.

Levelling-off of the OCR profile beginning at X = 0.43 contrasted the gradual increase in the PCR profile up to X = 1.5 (1.12 epoxy/amine ratio), suggesting fortification of the already stable polymer network. This fortification should minimize any rearrangement or redistribution of the PEI–E3–PEI network during metal extraction but could likely block or restrict metals to non-crosslinked $–NH_2$ and –NH sites. A detailed DRIFTS analysis of these sorbents, shown in the ESI,† supports these findings. Therein, beginning at X = 0.43 the decreasing 3288 ($–NH/–NH_2$)/2818 ($–CH_2$) and increasing 3120 ($–OH\cdots–NH/–NH_2$)/2818 IR absorbance profiles for cross-linked species levelled-off as the amine efficiency (mol CO_2 per mol N) gradually dropped. OCR values >100% in Fig. 1 could reflect a net sorbent mass gain of H_2O either strongly adsorbed within the sorbent pores or reacted with remaining E3 epoxy groups comprising the network.

The CO_2 capture and IR results predict that sorbents with X > 0.43 values would exhibit restricted metal adsorption performance while displaying only a marginal increase in leach resistance. Therefore, we further tested PES-0.43-100 for metal uptake. An initial packed-bed adsorption test of washed sorbent with ~250 ppm mixed La, Nd, Eu, Dy, and Yb (45–57 ppm each) solution yielded >99.9% recovery of the REE's (data not shown). Similarly, testing with simulated acid mine drainage solution (AMD-SYN; 49 ppb total REE, 1–14 ppm each) yielded >94.0% recovery of REE's, >99% removal of each Al, Mn, Fe, plus removal of Ni and Zn (data not shown). However, there was significant back-up of solution in the column during testing, especially with AMD-SYN, due to pressure drop across the small particles. This issue would be magnified at pilot-scale. Therefore, we adjusted the sorbent formulation to accommodate a 500 μm sorbent size.

Increased particle size of the sorbent inherently introduced slight mass transfer limitations during impregnation of the E3/PEI mixture. A 40 wt% instead of 50 wt% (100 μm sorbent) loading was required to minimize excessive accumulation of organics on the external SiO_2 surface, which causes agglomeration of the larger-size sorbent. Fig. 2 expectedly shows a similar trend in OCR values for the 500 μm as that for the 100 μm sorbents, with the same optimum E3/PEI ratio at X = 0.43.

Leach resistance of organic-functionalized sorbents is critical to prevent additional contamination of water sources and ensure longevity in practical application. Fig. 3(a) shows the PEI concentration profile while washing PES-0.43-500 prior to metal adsorption studies. These concentrations were determined using our previously-published UV-vis/Cu^{2+} aqueous amine quantification method.[37] Briefly, amine wash solution samples were diluted with ultrapure water; mixed (2 mL) with 500 ppm Cu^{2+} solution (2 mL); then scanned in a GENESYS IS 10 (Thermo Scientific) ultraviolet-visible spectrometer to determine aqueous amine concentration. The dramatic drop in PEI concentration from 2005 to 52 ppm after just 15 mL reflects loss of unreacted amines deposited

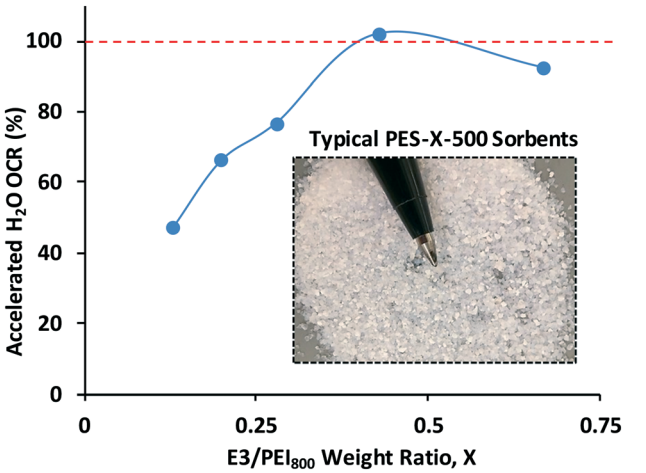

Fig. 2 OCR values for 500 μm, PES-X-500 sorbents. The inset picture shows the external morphology of the irregularly shaped particles.

on the external sorbent surface. Trailing of the PEI profile down to the limit of quantification at 600 mL represents gradual leaching of non-crosslinked amines from within the

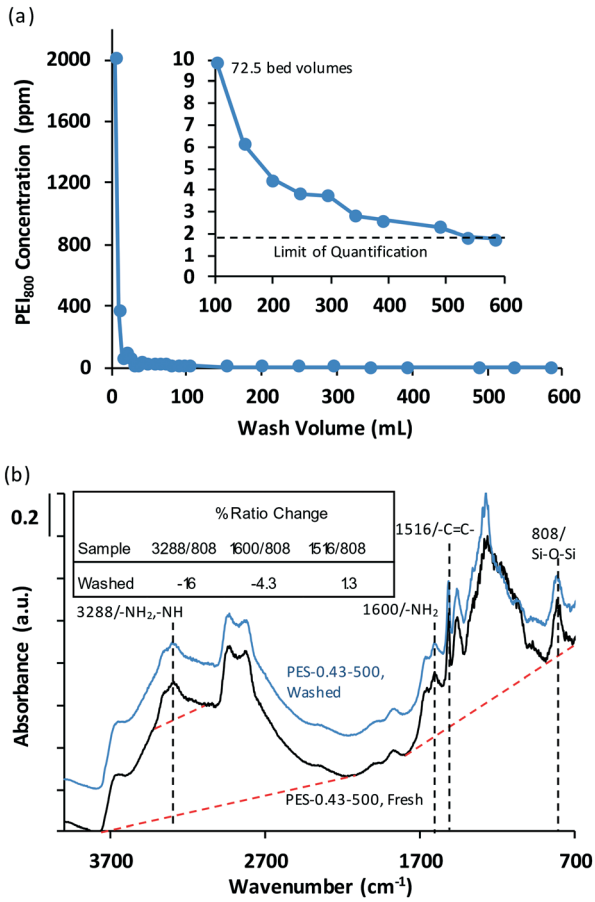

Fig. 3 (a) PEI_{800} concentration profile during PES-0.43-500 washing, determined by a UV-vis/Cu^{2+} technique. (b) DRIFTS absorbance spectra of fresh and washed sorbent, taken at 50 °C. Absorbance = log(1/I), where I is the single beam spectrum of each sample pretreated at 120 °C in N_2 for 30 min then cooled down.

sorbent pores. Calculating the OCR value from the spectroscopically verified PEI concentrations, OCR = wt% $Organic_{washed,UV\text{-}VIS}$/wt% $Organic_{fresh,TGA}$ × 100%, gave a value of 91.6% at 100 mL. This mirrors the same nitrogen content retained value (NCR) calculated by CHNS analysis and contrasts the 102.2% determined from the TGA method. This confirms the incorporation of H_2O into the polymer network presumably as either hydrogen bonded species or covalent vicinal diols, E3–CH_2–CH(OH)–CH_2(OH), through reaction with unreacted epoxies.

After 100 mL, the sorbent (0.5 g) was >99% stable towards additional washing. Accordingly, 700 mL of ultrapure water were used to pretreat a 3.5 g batch of PES-0.43-500 prior to water treatment studies. The DRIFTS spectra of this material in Fig. 3(b) show strong retention of all PEI and E3 IR features after washing. Slight reductions in the 3288 (amine)/808 (bulk silica Si–O–Si) and 1600/808 IR ratios were accompanied by a minimal increase in the –C═C–/Si–O–Si ratio. This affirms the slight loss of only amine previously determined by UV-vis/Cu^{2+}. Table 2 summarizes the OCR values and other associated physiochemical properties of the sorbent. The substantial ~60% reduction-growth in BJH pore volume-bulk density, minimal BET surface area loss, and shrinkage in BJH average pore size go with the >100% OCR (TGA) value after washing. Together these results support generation of E3–CH_2–CH(OH)–CH_2(OH) groups, which strengthen the network and provide added metal adsorption sites.

DRIFTS sequential impregnation

A diffuse reflectance FTIR, *in situ* impregnation study of SiO_2 with a surface layer (13 wt% total) and bulk layers (40 wt% total) of the epoxy/amine-0.43 mixture was conducted to gain detailed insight into the chemical structure of the optimum PES-0.43-500 sorbent. Fig. 4(a) top first shows the IR absorbance spectrum of a thin, crosslinked E3/PEI-0.43/1 film deposited onto a stainless-steel disk set atop the DRIFTS sample cup. This study provides the basis for assigning IR features produced by E3–PEI crosslinking within the PES sorbent. Here, about 5 μL of an 8 wt% E3/PEI (0.43/1)/MeOH solution were deposited onto the disk; MeOH evaporated at 40 °C for 60 min; and the resulting film heated to and reacted at 95 °C for 60 min then cooled down. After the reaction, negative N–H bands produced at 3360 and 3288 cm^{-1} (stretching), 1595 cm^{-1} (bending), and 950 to 650 cm^{-1} (wagging) for consumed –NH_2 and –NH groups[38–40] were accompanied by negative ones at 840 and 1255 cm^{-1} (C–O–C) plus 3100 to 2700 cm^{-1} (C–H stretching) for depleted epoxy groups.[39,41]

The generation of a positive broad O–H stretching band from 3600 to 2400 cm^{-1}, peaking at 3120 cm^{-1}, represents pendant hydroxyl groups from new E3–CH_2–CH(–**OH**)–CH_2–NH–PEI or E3–CH_2–CH(–**OH**)–CH_2–N–PEI segments. The region between 1550 and 900 cm^{-1} is convoluted with overlapping positive C–O (hydroxyls) and C–N (amine) stretching vibrations.[39,42,43] Therefore, we use the spectra of the pure E3 and PEI as a guide to assign the reactant and product groups. The band at 1357 cm^{-1} has been observed for other crosslinked amine–epoxy systems,[37,44] and is tentatively assigned as the coupling between the O–H bending from the hydroxyl groups and the C–H wagging of neighboring –CH.[43] The observed band at 1212 cm^{-1} was generated in our previous work for crosslinked E3–tetraethylenepentamine (TEPA) and shows C–N stretching of new E3–PEI species.[15] A strong vibration near this position was previously observed for triethylamine[39] and likely reflects tertiary amine species.

Note, 1212 cm^{-1} is outside the range typically observed for secondary alcohols.[43] Bands at 1089 and 1170 cm^{-1} could be produced by either C–N stretching of the crosslinks or C–O stretching of the alcohols.

Fig. 4(a), bottom shows that depositing a near monolayer of organics on the SiO_2 surface (13 wt%) diminished the IR band intensities of geminal (HO–Si–OH) and H-bonded (Si–OH···OH–Si) hydroxyls at 3738 and 3546 cm^{-1}, respectively. Simultaneously a strong, broad band from 3500 cm^{-1} to 2000 cm^{-1} and a weaker band at 1010 cm^{-1} for Si–OH···PEI species

Table 2 Physiochemical properties of optimum PES-0.43-500 and other sorbents. BDL, below detection limit, is <0.5 wt% and expected to be near 0 for SiO_2. Values for S930PLUS were provided by the manufacturer

	Support	Fresh sorbent	Washed sorbent		
Property	SiO_2–500	PES-0.43-500_Fresh	PES-0.43-500_Washed	Biochar-washed	S930PLUS
Organic loading (wt%)	3.4[a]	34.2	34.9		
Amine content (Wt% N; mmol N per g-sorb.)	BDL	8.52; 6.09	7.8; 5.57	BDL	
Moisture + CO_2 (wt%)	6.2	5.67	3.17	3.73	52–60
OCR – TGA		102.4			
OCR – UV-vis/Cu		91.5[b]	99[b]		
NCR – CHNS		91.5			
pH (10 wt% solids/H_2O)	4.8	10.3	9.0	9.7	11.4
ρ_{bulk} (g mL^{-1})	0.21	0.36	0.58	0.23	0.75
m^2 g^{-1} (BET)	300.4	136.9	125.2	273.4	
cm^3 g^{-1} (BJH)	2.9	1.18	0.48	0.057	
D_{pore}, avg. (nm)	13.8	12.3	5.8	1.79	

[a] Weight loss could be associated with removal of strongly adsorbed water and/or partial surface dehydroxylation. [b] OCR = wt% $Organic_{washed,UV\text{-}vis}$/wt% $Organic_{Fresh,TGA}$ × 100%.

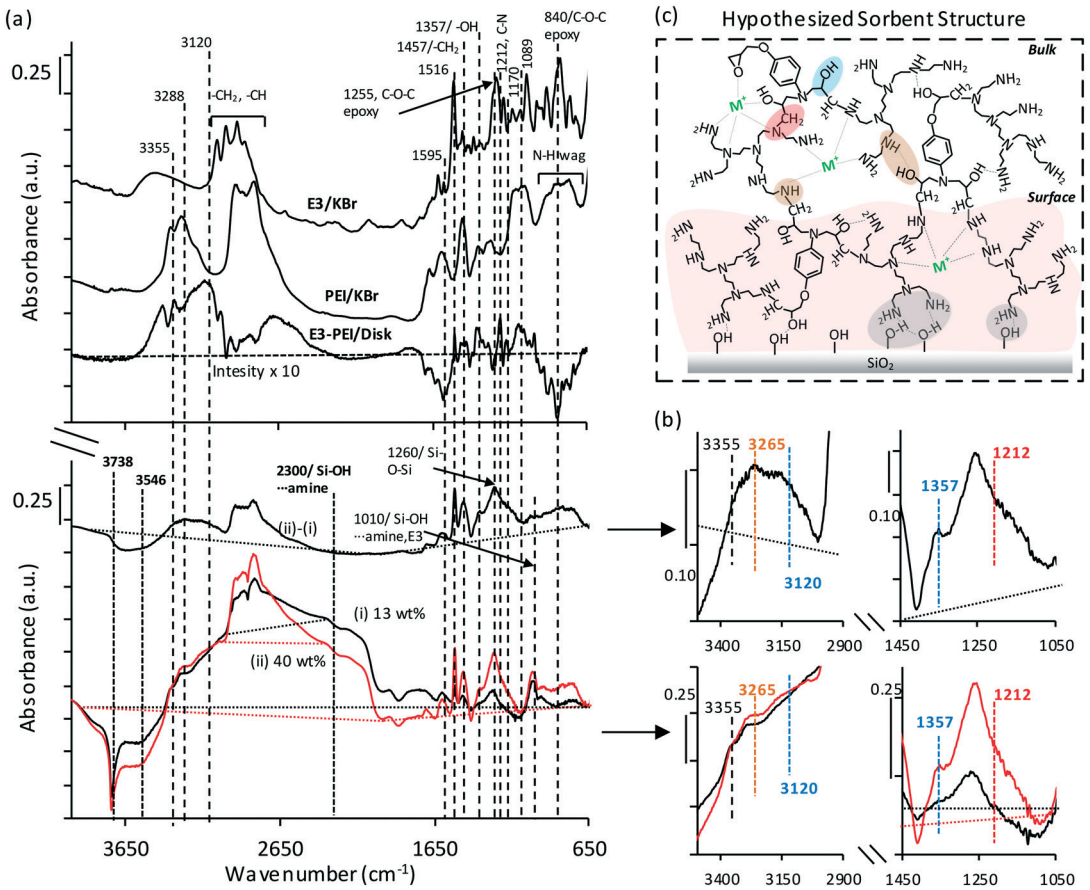

Fig. 4 (a) Top – IR absorbance spectra [Abs. = log(1/*I*)], of pure E3 and PEI deposited on KBr particles and absorbance spectrum of a crosslinked (95 °C, 60 min) E3/PEI-0.43/1 thin film deposited onto a metal disk; bottom – IR absorbance spectra of SiO_2 impregnated with surface (13 wt% total) and bulk (40 wt% total) layers of E3/PEI mixture at 40 °C following MeOH evaporation at 40 °C for 90 min and crosslinking at 105–110 °C for 60. Absorbance = log(I_0/*I*), where I_0 was the single beam spectrum of the pretreated SiO_2 bed and *I* were the single beam spectra of E3/PEI deposited onto the SiO_2 surface. Spectrum (iii)═(ii)–(i). (b) Magnification of key IR features for species formed from the E3–PEI reaction. (c) Hypothesized surface and bulk structures of the optimized PES-0.43-500 immobilized amine sorbent.

were produced.[45] Emergence of the structure-sensitive Si–O–Si band at 1260 cm^{-1} reflects slight changes in the bulk silica structure beneath the PEI–E3/SiO_2 interface. Distinctive –NH and –CH bands of PEI plus the –C═C– band of E3 affirms the organics were loaded onto silica. We previously observed all these IR features, minus those for E3, upon sequentially impregnating 13 wt% total PEI onto the same SiO_2 grade.[34]

Because of the net effect of positive band growth from loaded species and band reduction from reacted species, direct evidence for E3–PEI crosslinking at the interface is dubious. However, minimal growth in the 1357 cm^{-1} intensity shows only slight formation of pendant hydroxyls. This provides indirect evidence for marginal crosslinking near the silica interface. We expect that H-bonding of PEI with SiO_2 markedly inhibited amine groups from crosslinking with E3. Note that there are no clear IR features for covalent E3–silica linkages, presumably because of the typically slower reaction rate of epoxides with hydroxyls than with amines.

Loading the sorbent with an additional 27 wt% organics (40 wt% total) completed the remaining monolayer and deposited bulk layers of crosslinked E3–PEI species within the silica pores. The slight intensity drop for Si–OH sites paralleled with a 2.15-fold rise in the 2818 ($-CH_2$, –CH; PEI, E3)/2300 (Si–OH···amine) absorbance intensity ratio confirms coverage of the silica-bound E3–PEI surface layer. Fig. 4(b) highlights key spectral differences between the surface and bulk layers. These include broadened and/or strengthened features of amine and pendant hydroxyl groups between 3500 and 3000 cm^{-1}, along with enhanced formation of crosslinked species directly observed between 1400 and 1100 cm^{-1}. Increased 1357/1454 and 1212/1454 absorbance ratios by 79% and 319%, respectively, confirm higher concentrations of E3–CH_2–CH(–**OH**)–**CH_2**–**NH**–PEI and/or E3–CH_2–CH(–**OH**)–**CH_2**–**N**–PEI crosslinks present in the bulk than at the surface. Expectedly, the 1595/1454 ratio for previously unreacted –NH_2 dropped by 71%. Note, the 1516 (–C═C–)/1454 ratio diminished by 25% despite identical E3/PEI ratios for the bulk and surface. We attribute this to a shift in the spectral baseline. Because our other ratios change by ≫25%, conclusions drawn about their physical meaning are still valid.

Subtracting spectrum (i) from (ii) in Fig. 4(a) bottom yielded the chemical structure of primarily the bulk layers in spectrum (iii). Magnification of the IR features for this spectrum (and others) in Fig. 4(b) reveals suppression of the 3360 cm^{-1} band relative to the more pronounced features of the 3265 cm^{-1} band, which red-shifted from 3288 cm^{-1}. This suggests a relative gain in the amount of –NH (singlet peak) *versus* $–NH_2$ (doublet peak) groups upon crosslinking. Shifting of the amine band likely resulted from hydrogen bonding with proximal –OH groups. The broadened 1212 cm^{-1} C–N shoulder band and the more pronounced 1357 and 3120 cm^{-1} –OH bands further confirm the amine–epoxy reaction. These findings corroborate those based on the drop in the 1595/1454 ratio.

The *in situ* impregnation results show the sorbent is divided into two regions, according to Fig. 4(c). Region 1 consists of an interfacial near-monolayer of PEI and E3, primarily anchored to silica through Si–OH···PEI hydrogen bonds (geminal and H-bonded Si–OH) and minimally crosslinked by E3–PEI–E3 bridges. Region 2 constitutes a bulk network of epoxy–amine–epoxy (–C–N–C–) crosslinks that is further stabilized by amine–hydroxyl hydrogen bonds. We further postulate that a portion of unreacted E3 molecules in the surface layer migrated into the bulk for added crosslinking. Some expected sites for metal adsorption are also shown in the figure.

Heavy metal removal/recovery

Fig. 5 shows the adsorption of toxic heavy metals from a 125 ppm-concentrated, pH 6.2 (10–36 ppm each) solution by PES-0.43-500, organic pine biochar, and Purolite S930PLUS cation exchange resin. Our immobilized amine sorbent exhibited high affinities for cationic lead (98.2%), cadmium (88.6%), and mercury (99.0%) similarly as the biochar and ion exchange resin. Speciation diagrams of the metals calculated from stability constants at 25 °C suggest the following forms should be dominant: Pb^{2+} (major) and $Pb(OH)^{+}$ (minor);[46,47] Cd^{2+};[48] and $Hg(OH)_2^{0}$, which still possesses a partial positive charge on Hg.[49] Structures with –Cl instead of –OH groups are also viable. We ascribe adsorption of the Cd, Pb, and Hg

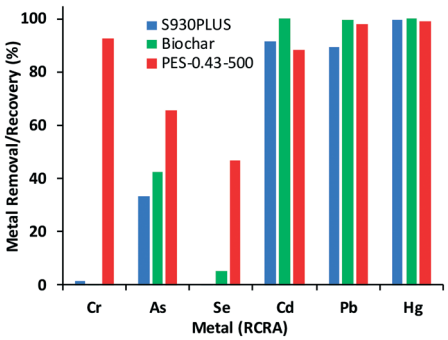

Fig. 5 Removal of toxic, aqueous cationic and oxyanionic RCRA heavy metals from a 160 ppm-concentrated solution at pH 6.24 by different sorbent types.

to complexation with the $–NH_2$/–NH (ref. 50) and –OH sites of the bulk E3–PEI network. Contrastingly, exchange of cationic Pb and Cd species with Na is the mechanism for S930PLUS. We expect a combination of ion exchange and surface complexation with oxygenated functional groups, like phenols and carboxylic acids, to dominate adsorption onto biochar.[51–53] Superior performance of PES-0.43-500 for removal of Cr^{6+} (92.9%), As^{5+} (65.7%), and Se^{6+} (47.0%) in oxyanionic forms highlights the unique feature of the PEI–E3 network to simultaneously adsorb positively and negatively charged species. Expected dominant forms of the aqueous metals include $HCrO_4^{-}$ and CrO_4^{2-} (both major);[54] $H_2AsO_4^{-}$ and $HAsO_4^{2-}$ (both major);[55] and SeO_4^{2-}.[56,57] Because PES-0.43-500 and S930PLUS are basic, shifting of the local solution pH within the sorbent bed during testing could give CrO_4^{2-} as the dominant form of chromium. We attribute adsorption of Cr by PES-0.43-500 to a combination of (a) amine oxidation–Cr(VI) reduction to form amides, imides–Cr(III) followed by Cr (III)···amide, imide chelation and (b) chromate···$_2$HN–, HN–, HO– electrostatic interactions.[58] Similar schemes are envisioned for As and Se adsorption.

Failure of S930PLUS to adsorb Cr and Se is unsurprising considering the metal compounds' anionic nature. Adsorption of As by the resin suggests positive characteristics of the compound. We postulate that coordination of arsenate to Pb or Cd facilitated exchange with the Na ions. High uptake percentages of these six metals from stable single-element solutions (Fig. S3, ESI†) similarly as for the mixed solutions eliminates physical filtration as a mechanism of their removal.

Fig. 6(a) shows the performance of each sorbent for heavy metal remediation from authentic flue gas desulfurization water discharge derived from the treatment of coal combustion exhaust gas. PES-0.43-500 exhibited similar uptake of Hg (85.9%) and Pb (72.3%) compared to biochar and S930PLUS. Appreciable amounts of Cr (50.3%) and some Se (17.0%) were removed by our sorbent whereas these metals (except Se by S930PLUS, 13.9%) were ignored by the other materials. We further observed comparable removal of Al (97.7%-below reporting limit), Mn, and Ni. Interestingly, we achieved superior removal of uranium (U, non-radioactive) and rhenium (Re) down to below their reporting limits. Rhenium was previously used as a surrogate for radioactive technetium, ^{99}Tc, in metal removal research conducted by us and others.[59–61] Adsorption of both U and Re suggests that BIAS sorbents could be used for radioactive applications, like cleaning superfund sites. A relatively lower proportion of Cd (63.5%)/Cr, and Cd/Pb adsorption from FGD by our sorbent compared to from the ideal 6-element RCRA solution could be owed to competitive adsorption between lower acidity Cd–H_2O complexes and those with higher acidities, like Cu, Zn, and Ni hydrates. Quantum chemical modelling of and experimental results for $[Cd(H_2O)_6]^{2+}$, $^{2}[Cu(H_2O)_6]^{2+}$, $[Zn(H_2O)_6]^{2+}$, and $^{3}[Ni(H_2O)_6]^{2+}$ complexes respectively gave corresponding pK_a's of 10.0, 8, and 9.0, and 9.6.[62] SEM images, shown in Fig. S4 of the ESI,† reveal no appreciable

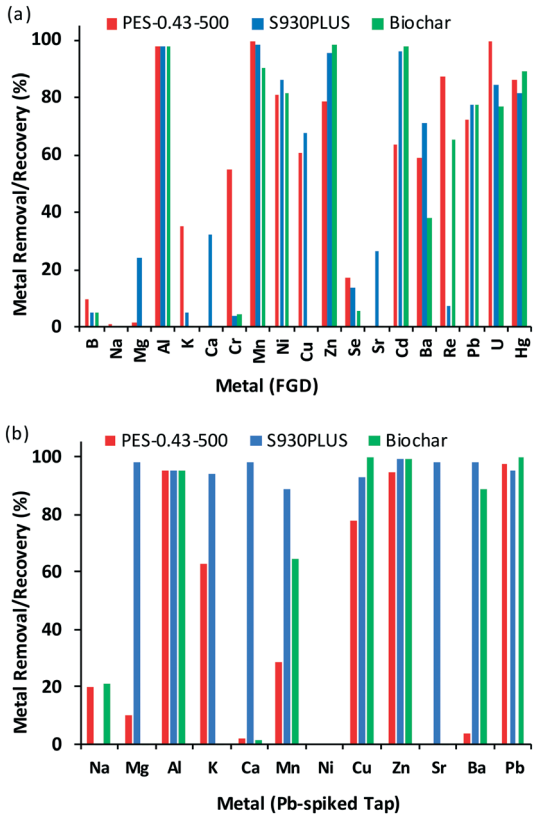

Fig. 6 Removal of RCRA and other heavy metals from (a) flue gas desulfurization water – 2606 ppm alkali/alkaline metals, 121.3 ppm heavy metals, 1.6 ppb REEs, pH 6.7; and (b) 125 ppb Pb-spiked tap water – 81.0 ppm alkali/alkaline metals, 1.21 ppm heavy metals, pH 5.7 by different sorbent types.

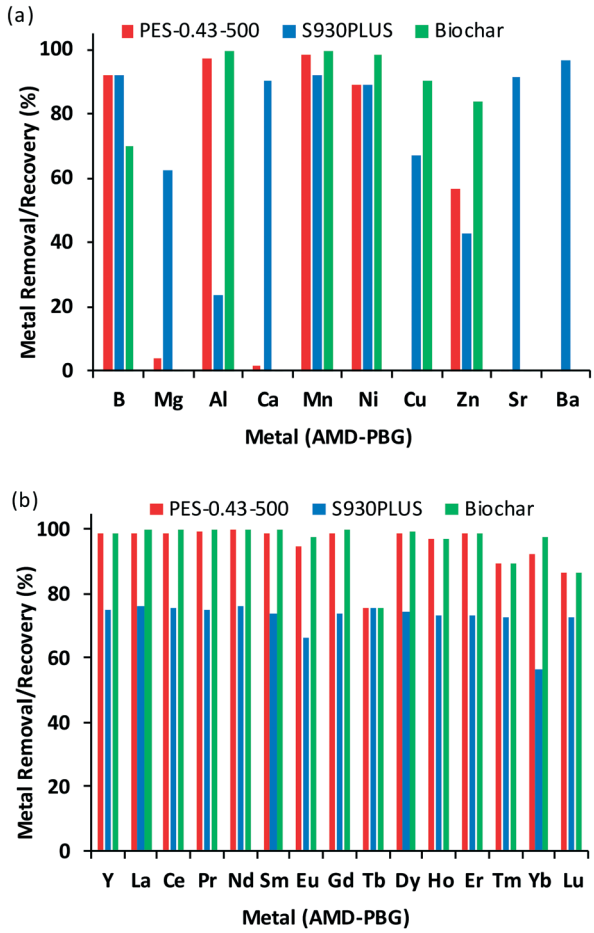

Fig. 7 Removal/recovery of (a) heavy metals and (b) rare earth elements (REEs) from a local acid mine drainage sample – 68.2 ppm alkali plus alkaline metals, 7.5 ppm heavy metals, 63.6 ppb REEs, pH 3.6, fouling (alkali + alkaline + heavy)/REE ratio of 1191/1.

change in the sorbent's structure upon adsorbing metals from this real FGD. The lack of swelling implicates stable flow-through properties during cycling. This contrasts column plugging observed in our previous work, involving unsupported pure polymers.

Fig. 6(b) shows 97.6% removal of Pb from spiked tap water, which dropped the excessively high starting concentration from 125 down to 2.96 ppb. This is below the 15 ppb regulatory limit set by the US Environmental Protection Agency (EPA). Along with Pb, the immobilized amine sorbent further removed most Zn (94.6%) and much of the Cu (77.4%) like the other sorbents. S930PLUS displayed superior metal removal performance for this tap water sample (Ca = 33.7 ppm, "moderately hard"),[63] with additional Ba and Sr cation uptake. However, samples with "very hard" Ca content of 251 to 1120 ppm $CaCO_3$ (100 to 448 ppm Ca) and high Mg should diminish the resins long-term effectiveness to capture Pb and other toxic species due to competitive adsorption.

Acid mine drainage from coal mines is a large source of both terrestrial water contamination and precious rare earth elements, both of which are research focuses for the U.S. Department of Energy.[18] Fig. 7 shows the performance of the sorbents to remove/recover heavy metals/REE's from local acid mine drainage runoff at pH 3.6. PES-0.43-500 expectedly displayed good affinities for Ni, Mn, and Al plus B (91.8%-below reporting limit), as shown in Fig. 7(a). The BIAS sorbent favored the removal of both B and Al, whereas B uptake was lowest for biochar and Al uptake was lowest for S930PLUS. Relatively high boron uptake is advantageous towards addressing the health advisory issued by the EPA regarding B in drinking water, which could be contaminated by AMD runoff.[64] Interestingly, our sorbent (and biochar) displayed significantly higher REE uptakes of 86–99.9% compared to 56.3–76.1% for the ion exchange resin (Fig. 7(b)). We attribute the inferior performance of S930PLUS to strong competitive adsorption between the ppb-level REE's and ppm-level Mg and Ca cations. We additionally treated AMD-PBG with commercial activated carbon (Calgon, 1235.7 m^2 g^{-1}) under identical flowing conditions. Inferior adsorption of essentially all metals, except Sr and Yb, by the high-surface area carbon in Fig. S5 in the ESI† compared to PES-0.43-500 further positions the BIAS as a competitive water treatment technology.

The general behavior for metal capture by PES-0.43-500 followed as: REEs (89.4 to 99.9%) ~ Al (97.5%) > Zn (56.9%) > Mg (3.7%) > Sr (0%). This mirrored the trend in the aqueous metals' acidities, as characterized by pK_a values of their hydrated complexes: La to Yb (5.88 to 3.53) ~ Al (4.6) < Zn (9.0) < Mg (11.2–10.5) < Sr (13.3).[62,65] This strong correlation implies that acid–base interactions are a critical driving force for metal adsorption onto immobilized amine sorbents.

Although biochar seemed to perform as well as PES-0.43-500 for REE's and heavy metals regarding different water sources, Table 3 shows that the relative maximum uptakes of Cr (heavy metal oxyanion), Cd (heavy metal cation), and Eu (REE cation) from pure solutions at their natural pH were significantly higher for our material than the carbon-based ones. Testing of activated carbon for maximum uptakes revealed that the immobilized amine sorbent was still far superior, despite the high surface area of the carbon. The lack of competitive adsorption between Cd or Eu and alkaline species (Mg, Ca, *etc.*) in the single-element ideal solutions facilitated their highest maximum uptakes for S930PLUS. However, the lack of Cr adsorption highlights the drawback of cationic IER to remove some toxic anionic species.

Unexpectedly, spiking the 5.0 mM cation solutions with an equimolar amount of SO_4^{2-} or NO_3^- anion generally produced modest rises in both Cd^{2+} and Eu^{3+} uptake for our PES-0.43-500, by a factor of 1.2 to 1.5. However, Eu^{3+} uptake in the presence of SO_4^{2-} jumped by a factor of 3.0. Furthermore, while the sorbent displayed negligible affinity for the anions alone (5.0 mM uptake test, data not shown), uptake of SO_4^{2-} was 7.8 and 14.6 wt% with Cd and Eu, respectively, while NO_3^- was between 4 and 5 wt%. These results suggest that electrostatic interactions between cations and anions in solution increased the overall affinity of Cd^{2+} and Eu^{3+} to the amine sites, whereby the chelated cations further adsorbed the anions.

PES-0.43-500 showed better uptake of Cd than NNN-S and IIIP-AAAPTS/SiO_2 from the literature, yet uptakes of Cr and Eu below those of the other functionalized silica sorbents. However, the nano-size of MNPs/SiO_2-AMPA makes them unsuitable for practical packed-bed systems due to undoubtedly high pressure drop. Additionally, the prohibitively high cost of $476/25 g for 1-(2-pyridylazo) 2-naphthol (0.1 kg scale) *versus* the low costs of $396/1000 g for PEI_{800} and $140/305 g for E3 makes the PAN/APTES modified Sil sorbent impractical for commercialization. Proven and marketable fixed-bed water treatment systems can be easily modified to accommodate our low-cost PES-0.43-500, $55 per kg (materials cost, 1 MT scale), providing a cost-effective water remediation technique. Note that material costs can decrease by orders of magnitude as manufacturing quantities increase.

The DRIFTS spectra of PES-0.43-500 samples with these adsorbed metals in Fig. S6 of the ESI† clearly show oxidation of the amines to amides/imides by captured chromate, and interaction of PEI with Cd^{2+} and Eu^{3+} through $-NH_2$/–NH···metal interactions. This supports our previous hypothesis for heavy metal removal. Participation of the –OH groups during adsorption was expected but not clearly observed from the IR spectra.

Cyclic recover-strip testing of PES-0.43-500 was performed with a synthetic acid mine drainage solution (AMD-SYN, pH 2.6) for metal adsorption and a pH 8.5 ammonium hydroxide–ammonium citrate buffer for subsequent metal stripping and sorbent regeneration. AMD-SYN was more acidic and had a higher fouling metal (alkali + alkaline + heavy)/REE ratio of 12 892/1 than that of 1191/1 for authentic AMD-PBG. Fig. 8 shows high stability of the sorbent to extract heavy metals, especially REE's, from highly contaminated AMD-SYN solution. Like adsorption from AMD-PBG the sorbent displayed high affinities for Fe, Al, and Mn plus Cr (62.2%-below reporting limit, cycle 1) in Fig. 8(a) which only slightly dropped to 52.5% after cycle 5. Moreover the REE's displayed consistently excellent uptakes of 79.2 to 99.2%, despite the somewhat erratic behavior of La. Minimal recovery of Na, Mg, and Ca shows negligible competitive adsorption between toxic or valuable metals and inert

Table 3 Relative maximum uptake of Cr, Cd, and Eu from single-element solutions at their natural pH by our best sorbent after 17–24 hours under agitation, compared with the commercially available sorbents and other functionalized-silica materials in the literature

Sorbent name	Sorb. dose (mg mL^{-1} soln.)	Metal conc. (mM)	Relative maximum uptake (wt%)/natural pH			Ref.
			Cr	Cd	Eu	
PES-0.43-500	150/50	5.0	0.76/7.7	8.78/5.1	6.25/5.0	This work
PES-0.43-500 (with SO_4^{2-}:NO_3^-)	150/50	5.0		11.8 : 9.9	17.9 : 7.8	
Biochar	150/50	5.0	0/7.7	2.02/5.1	1.84/5.0	
S930PLUS	150/50	5.0	0/7.7	13.05/5.1	11.26/5.0	
Activated carbon	150/50	5.0	0.53/7.7	0.25/5.1	2.52/5.0	
MNPs[a]/SiO_2-AMPA[b]	100/30	2			6.9/7.0	66
PAN[c]/APTES[d] modified Sil	1000/1000	0.99			13.0/4.0	67
NNN[e]-S	100/10	0.8–0.9	1.3/6.0	2.2/6.0		68
IIP-AAAPTS[f]/SiO_2	50/50	0.68		5.7		69

[a] Magnetic nanoparticles. [b] Aminomethylenephosphonic acid. [c] 1-(2-Pyridylazo) 2-naphthol. [d] 3-Aminopropyl triethoxysilane. [e] [(2-Aminoethylamino)ethylamino]propyltrimethoxysilane. [f] 3-[2-(2-Aminoethylamino)ethylamino]propyltrimethoxysilane.

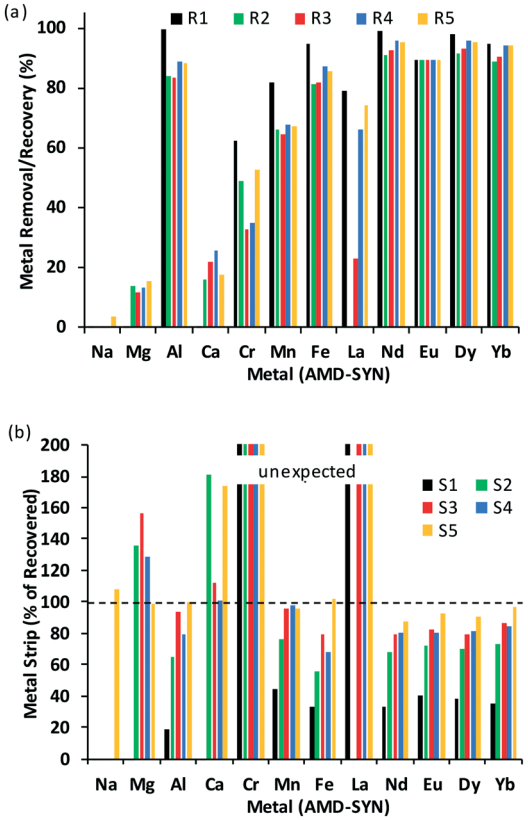

Fig. 8 Cyclic metal recover-strip (a) and (b) testing with synthetic acid mine drainage, AMD-SYN – 354 ppm alkali plus alkaline metals, 341 ppm heavy metals, 53.9 ppb REEs, pH 2.6, fouling (alkali + alkaline + heavy)/REE ratio of 12 892/1.

species. These results are similar to those we previously observed for porous E3–tetraethylenepentamine (TEPA) monolith[15] and PEI–acrylamide/SiO_2 hybrid hydrogel sorbent particles[70] (except Mg recovery by hydrogel). Gradually improved stripping performance of the buffer during cycling, shown in Fig. 8(b) could reflect a decreasing amount of irreversibly adsorbed species on the sorbent. The ≫100% stripping of recovered Cr (5.29 ppm fresh, 14–21 ppm stripped) and La is unclear and under investigation.

To gain a better understanding of the sorbent's performance towards heavy metals (Al, Mn, Cu, Zn, Cd) and REEs (La, Nd, Eu, Dy, Yb) present in a variety of water sources, we performed a kinetic uptake test by flowing 40 mL of a 10.0 mM equimolar metal solution (natural pH 3.9) over 0.5 g of PES-0.43-500 at 0.5 mL min^{-1} and sampling every 1 mL (2 min). Results in Fig. S7 of the ESI† confirmed that both uptake kinetics (mmol M^+ g^{-1} min^{-1}) and capacity (mmol M^+ g^{-1}) grew across the Ln^{3+} series as both ionic radii and pK_a dropped. Disregarding Cd, the heavy metals displayed similar behavior as the REEs. Herein, both kinetics and capacity followed as: Al (aqueous ionic radii 50 pm) > [Cu (72 pm, pK_a 7.7), Zn (70 pm, 5.5)] > Mn (80 pm). These capacity trends held true upon cross-comparing heavy metals-REEs, like Al-Nd (50–108 pm) at similar pK_a. These results highlight the importance of considering cation content, size, and acidity when refining sorbent formulations to treat specific water sources.

Conclusions

Basic immobilized amine sorbents (BIAS), utilizing robust amine–epoxide cross-linkages, were prepared as H_2O-stable materials to remove/recover a myriad of toxic heavy metals and rare earth elements from ideal and authentic water sources. Optimization of the *N-N*-diglycidyl-4-glycidyloxyaniline (E3, epoxy)/polyethylenimine (PEI, amine) ratio (0.43) within a silica support (40% loading) endowed the sorbent with a 99% leach resistance of its polymer network after prewashing. Diffuse reflectance FTIR confirmed this network was comprised of (i) a hydrogen-bonded E3/PEI···silica interfacial layer surrounded by (ii) a crosslinked E3–PEI bulk structure. Relative to other commercial sorbents, we observed equal or superior performance of our material to remove toxic (Pb, Cd, Hg, Cr, As, Se), heavy (Al, Mn, Ni, Zn, Cu, Re, others), and valuable (La through Yb REE's) metals from an ideal solution, tap water, flue gas desulfurization water, and acid mine drainage. Solution pH values ranged from 2.6 (acidic) to 6.7 (near-neutral). Exceptional among these sorbent types, the BIAS simultaneously removed toxic cationic and oxyanionic (CrO_4^{2-}, $HAsO_4^{2-}$, SeO_4^{2-}) species while largely neglecting Na, Ca, and Mg. Future work involves changing the amine type or stripping solution to tune the adsorptive or desorptive selectivity towards toxic/semi-toxic metals or REE's.

Disclaimer

This work was funded by the Department of Energy, National Energy Technology Laboratory, an agency of the United States Government, through a support contract with Leidos Research Support Team (LRST). Neither the United States Government nor any agency thereof, nor any of their employees, nor LRST, nor any of their employees, makes any warranty, expressed or implied, or assumes any legal liability or responsibility for the accuracy, completeness, or usefulness of any information, apparatus, product, or process disclosed, or represents that its use would not infringe privately owned rights. Reference herein to any specific commercial product, process, or service by trade name, trademark, manufacturer, or otherwise, does not necessarily constitute or imply its endorsement, recommendation, or favoring by the United States Government or any agency thereof. The views and opinions of authors expressed herein do not necessarily state or reflect those of the United States Government or any agency thereof.

Conflicts of interest

This work is, in part, incorporated into a published patent application that was licensed by a commercial entity: Stable Immobilized Amine Sorbents for REE and Heavy Metal

Recovery from Liquid Sources, Appl. # 15/782315. This license agreement was publicly disclosed by DOE. Some of the authors of this manuscript, DOE, and the commercial entity could financially be impacted by this work.

Acknowledgements

This work was performed in support of the US Department of Energy's Fossil Energy Crosscutting Technology Research Program. The Research was executed through the NETL Research and Innovation Center's Water Management for Power Systems project. Research performed by Leidos Research Support Team staff was conducted under the RSS contract 89243318CFE000003. This research was supported in part by an appointment to the National Energy Technology Laboratory Research Participation Program, sponsored by the U.S. Department of Energy and administered by the Oak Ridge Institute for Science and Education. We thank Vyacheslav Romanov for use of the DRIFTS. We thank Karen Johnson, Bill Garber, Phil Tinker, and Rob Thompson for performing ICP-MS, ICP-OES, CHNS, and CVAAS sample analyses.

References

1 C. Charles, It's another Flint Situation' – Pullman Apartment Complex Dealing with Bad Water, Fox 17 West Michigan [online] June 6, 2018, https://fox17online.com/2018/06/06/its-another-flint-situation-pullman-apartment-complex-dealing-with-bad-water/, (accessed Aug. 1, 2018).

2 B. Finley, Drinking Water in Three Colorado Cities Contaminated with Toxic Chemicals Above EPA Limits, The Denver Post [online] July 25, 2017, https://www.denverpost.com/2017/07/25/air-force-admits-soil-water-contamination/, (accessed Sept. 30, 2016).

3 K. Matheny, Scientists Puzzled by Mercury's Jump in Great Lakes Fish. Detroit Free Press [online] March 24, 2017, https://www.freep.com/story/news/local/michigan/2017/03/24/mercury-rising-scientists-puzzled-metals-jump-great-lakes-fish/99306786/", (accessed Aug. 1, 2018).

4 U.S. Geological Survey, Study Estimates about 2.1 Million People using Wells High in Arsenic, [online] Oct. 18, 2017, https://www.usgs.gov/news/study-estimates-about-21-million-people-using-wells-high-arsenic, (accessed Jan. 31, 2019).

5 The Woods Hole Oceanographic Institution, Fukushima Radiation [online], https://www.whoi.edu/know-your-ocean/ocean-topics/pollution/fukushima-radiation/, (accessed June 21, 2018).

6 U.S. Environmental Protection Agency, Ground Water and Drinking Water-National Primary Drinking Water Regulation [online], https://www.epa.gov/ground-water-and-drinking-water/national-primary-drinking-water-regulations#Inorganic, (accessed Jan. 31, 2018).

7 U.S. Environmental Proetction Agency, Electronic Code of Federal Regulations (CFR), Part 141 - National Primary Drinking Water Regulations, Subpart I - Control of Lead and Copper, National Service Center for Environmental Publications [online] 1995, https://nepis.epa.gov/Exe/ZyNET.EXE?ZyActionL=Register&User=anonymous&Password=anonymous&Client=EPA&Init=1, (accesed Jan. 31, 2018).

8 U.S. Environmental Protection Agency, Office of Water, Final Aquatic Life Ambient Water Quality Criteria for Aluminum - 2018 [online], https://www.epa.gov/wqc/aquatic-life-criteria-aluminum, (accessed Jan. 31, 2019).

9 N. F. Gray, Acid mine drainage composition and the implications for its impact on lotic systems, *Water Res.*, 1998, **32**(7), 2122–2134.

10 M. Olías, C. R. Cánovas, M. D. Basallote, F. Macías, R. Pérez-López, R. M. González, R. Millán-Becerro and J. M. Nieto, Causes and impacts of a mine water spill from an acidic pit lake (Iberian Pyrite Belt), *Environ. Pollut.*, 2019, **250**, 127–136.

11 L. F. O. Silva, M. Wollenschlager and M. L. S. Oliveira, A preliminary study of coal mining drainage and environmental health in the Santa Catarina region, Brazil, *Environ. Geochem. Health*, 2011, **33**(1), 55–65.

12 Y. H. Huang, P. K. Peddi, C. Tang, H. Zeng and X. Teng, Hybrid zero-valent iron process for removing heavy metals and nitrate from flue-gas-desulfurization wastewater, *Sep. Purif. Technol.*, 2013, **118**, 690–698.

13 R. Abel and A. Phillips, Groundwater Contamination from Texas Coal Ash Dumps. EarthJusticeEnvironmental, Integrity Project [online] Jan. 17, 2019, https://earthjustice.org/, (accessed Jan. 1, 2019).

14 Rare Earths - Statistics and Information, U.S. Geological Society [online] 2015, http://minerals.usgs.gov/minerals/pubs/commodity/rare_earths/, (accessed Jan. 1, 2016).

15 W. C. Wilfong, B. W. Kail, T. L. Bank, B. H. Howard and M. L. Gray, Recovering Rare Earth Elements from Aqueous Solution with Porous Amine-Epoxy Networks, *ACS Appl. Mater. Interfaces*, 2017, **9**(21), 18283–18294.

16 H. Zhang, R. G. McDowell, L. R. Martin and Y. Qiang, Selective Extraction of Heavy and Light Lanthanides from Aqueous Solution by Advanced Magnetic Nanosorbents, *ACS Appl. Mater. Interfaces*, 2016, **8**(14), 9523–9531.

17 Z. Zhao, X. Sun and Y. Dong, Synergistic Effect of Doped Functionalized Ionic Liquids in Silica Hybrid Material for Rare Earth Adsorption, *Ind. Eng. Chem. Res.*, 2016, **55**(7), 2221–2229.

18 D. Bauer, *et al.*, U.S. Department of Energy, U.S. Department of Energy Critical Materials Strategy, Office of Policy [online] December, 2010, https://www.energy.gov/policy/downloads/2010-critical-materials-strategy, (accessed 7/9/2019).

19 J. C. Callura, K. M. Perkins, C. W. Noack, N. R. Washburn, D. A. Dzombak and A. K. Karamalidis, Selective adsorption of rare earth elements onto functionalized silica particles, *Green Chem.*, 2018, **20**(7), 1515–1526.

20 Z. Weng, N. Haque, G. M. Mudd and S. M. Jowitt, Assessing the energy requirements and global warming potential of the production of rare earth elements, *J. Cleaner Prod.*, 2016, **139**, 1282–1297.

21 E. Monazam, R. Siriwardane, D. Miller and D. McIntyre, Rate analysis of sorption of Ce3+, Sm3+, and Yb3+ ions from

aqueous solution using Dowex 50W-X8 as a sorbent in a continuous flow reactor, *J. Rare Earths*, 2018, 648–655.

22 R. K. Nekouei, F. Pahlevani, M. Assefi, S. Maroufi and V. Sahajwalla, Selective isolation of heavy metals from spent electronic waste solution by macroporous ion-exchange resins, *J. Hazard. Mater.*, 2019, **371**, 389–396.

23 J. Wen, Y. Yi and G. Zeng, Effects of modified zeolite on the removal and stabilization of heavy metals in contaminated lake sediment using BCR sequential extraction, *J. Environ. Manage.*, 2016, **178**, 63–69.

24 K.-M. Poo, E.-B. Son, J.-S. Chang, X. Ren, Y.-J. Choi and K.-J. Chae, Biochars derived from wasted marine macro-algae (Saccharina japonica and Sargassum fusiforme) and their potential for heavy metal removal in aqueous solution, *J. Environ. Manage.*, 2018, **206**, 364–372.

25 I. Enniya, L. Rghioui and A. Jourani, Adsorption of hexavalent chromium in aqueous solution on activated carbon prepared from apple peels, *Sustainable Chem. Pharm.*, 2018, **7**, 9–16.

26 P. Li, J. Wang, X. Li, W. Zhu, S. He, C. Han, Y. Luo, W. Ma, N. Liu and D. D. Dionysiou, Facile synthesis of amino-functional large-size mesoporous silica sphere and its application for Pb2+ removal, *J. Hazard. Mater.*, 2019, **378**, 120664.

27 J. Florek, A. Mushtaq, D. Lariviere, G. Cantin, F.-G. Fontaine and F. Kleitz, Selective recovery of rare earth elements using chelating ligands grafted on mesoporous surfaces, *RSC Adv.*, 2015, **5**(126), 103782–103789.

28 J. Roosen, J. Spooren and K. Binnemans, Adsorption performance of functionalized chitosan-silica hybrid materials toward rare earths, *J. Mater. Chem. A*, 2014, **2**(45), 19415–19426.

29 M. Ghoul, M. Bacquet and M. Morcellet, Uptake of heavy metals from synthetic aqueous solutions using modified PEI —silica gels, *Water Res.*, 2003, **37**(4), 729–734.

30 A. L. Roes, L. B. Tabak, L. Shen, E. Nieuwlaar and M. K. Patel, Influence of using nanoobjects as filler on functionality-based energy use of nanocomposites, *J. Nanopart. Res.*, 2010, **12**(6), 2011–2028.

31 H. A. Alhashimi and C. B. Aktas, Life cycle environmental and economic performance of biochar compared with activated carbon: A meta-analysis, *Resour., Conserv. Recycl.*, 2017, **118**, 13–26.

32 R. D. Bergman, H. Gu, S. Page-Dumroese and N. M. Anderson, in *Life cycle analysis of biochar*, Cambridge University Press, Cambridge, UK, 2017, ch. 3.

33 W. C. Wilfong, B. W. Kail and M. L. Gray, Rapid Screening of Immobilized Amine CO2 Sorbents for Steam Stability by Their Direct Contact with Liquid H2O, *ChemSusChem*, 2015, **8**(12), 2041–2045.

34 W. C. Wilfong, B. W. Kail, C. W. Jones, C. Pacheco and M. L. Gray, Spectroscopic Investigation of the Mechanisms Responsible for the Superior Stability of Hybrid Class 1/Class 2 CO2 Sorbents: A New Class 4 Category, *ACS Appl. Mater. Interfaces*, 2016, **8**(20), 12780–12791.

35 Y. G. Ko, S. S. Shin and U. S. Choi, Primary, secondary, and tertiary amines for CO2 capture: Designing for mesoporous CO2 adsorbents, *J. Colloid Interface Sci.*, 2011, **361**(2), 594–602.

36 Y. Zhai and S. S. C. Chuang, The Nature of Adsorbed Carbon Dioxide on Immobilized Amines during Carbon Dioxide Capture from Air and Simulated Flue Gas, *Energy Technol.*, 2017, **5**(3), 510–519.

37 W. C. Wilfong, B. W. Kail, Q. Wang and M. L. Gray, Novel Rapid Screening of Basic Immobilized Amine Sorbent/Catalyst Water Stability by a UV/Vis/Cu(2+) Technique, *ChemSusChem*, 2018, **11**(23), 4114–4122.

38 D. D. Miller and S. S. C. Chuang, The Effect of Electron-Donating Groups and Hydrogen Bonding on H2S Capture over Polyethylene Glycol/Amine Sites, *J. Phys. Chem. C*, 2016, **120**(2), 1147–1162.

39 N. B. Colthup, *et al.*, *Introduction to Infrared and Raman Spectroscopy*, Acedemic Press, Inc., New York, NY, 2nd edn, 1975.

40 W. C. Wilfong, C. S. Srikanth and S. S. Chuang, In situ ATR and DRIFTS studies of the nature of adsorbed CO(2) on tetraethylenepentamine films, *ACS Appl. Mater. Interfaces*, 2014, **6**(16), 13617–13626.

41 E. Schab-Balcerzak, H. Janeczek, B. Kaczmarczyk, H. Bednarski, D. Sęk and A. Miniewicz, Epoxy resin cured with diamine bearing azobenzene group, *Polymer*, 2004, **45**(8), 2483–2493.

42 J. E. Stewart, Vibrational spectra of primary and secondary aliphatic amines, *J. Chem. Phys.*, 1959, **30**(5), 1259–1265.

43 R. M. Silverstein, *Spectrometric Identification of Organic Compounds*, John Wiley & Sons, Inc., Hoboken, 2005.

44 M. E. Silva, S. S. Chakravartula and S. C. Chuang, Silica-Supported Amine Catalysts for Carbon–Carbon Addition Reactions, *Top. Catal.*, 2012, **55**(7–10), 580–586.

45 F. H. Van Cauwelaert, F. Vermoortele and J. B. Uytterhoeven, Infra-red spectroscopic study of the adsorption of amines on the A-type and B-type hydroxyls of an aerosil silica gel, *Discuss. Faraday Soc.*, 1971, **52**(0), 66–76.

46 J. Powell Kipton, L. Brown Paul, H. Byrne Robert, T. Gajda, G. Hefter, A.-K. Leuz, S. Sjöberg and H. Wanner, Chemical speciation of environmentally significant metals with inorganic ligands. Part 3: The Pb2+ + OH–, Cl–, CO32–, SO42–, and PO43– systems (IUPAC Technical Report), *Pure Appl. Chem.*, 2009, **81**, 2425.

47 O. Allahdin, J. Mabingui, M. Wartel and A. Boughriet, Removal of Pb2+ ions from aqueous solutions by fixed-BED column using a modified brick: (Micro)structural, electrokinetic and mechanistic aspects, *Appl. Clay Sci.*, 2017, **148**, 56–67.

48 J. Powell Kipton, L. Brown Paul, H. Byrne Robert, T. Gajda, G. Hefter, A.-K. Leuz, S. Sjöberg and H. Wanner, Chemical speciation of environmentally significant metals with inorganic ligands. Part 4: The Cd2+ + OH–, Cl–, CO32–, SO42–, and PO43– systems (IUPAC Technical Report), *Pure Appl. Chem.*, 2011, **83**, 1163.

49 J. Powell Kipton, L. Brown Paul, H. Byrne Robert, T. Gajda, G. Hefter, S. Sjöberg and H. Wanner, Chemical speciation of environmentally significant heavy metals with inorganic ligands. Part 1: The Hg2+− Cl−, OH−, CO32−, SO42−, and PO43− aqueous systems (IUPAC Technical Report), *Pure Appl. Chem.*, 2005, **77**, 739.

50 P. Di Bernardo, P. L. Zanonato, A. Melchior, R. Portanova, M. Tolazzi, G. R. Choppin and Z. Wang, Thermodynamic and Spectroscopic Studies of Lanthanides(III) Complexation with Polyamines in Dimethyl Sulfoxide, *Inorg. Chem.*, 2008, **47**(3), 1155–1164.

51 H. Li, X. Dong, E. B. da Silva, L. M. de Oliveira, Y. Chen and L. Q. Ma, Mechanisms of metal sorption by biochars: Biochar characteristics and modifications, *Chemosphere*, 2017, **178**, 466–478.

52 F. Zhang, X. Wang, D. Yin, B. Peng, C. Tan, Y. Liu, X. Tan and S. Wu, Efficiency and mechanisms of Cd removal from aqueous solution by biochar derived from water hyacinth (Eichornia crassipes), *J. Environ. Manage.*, 2015, **153**, 68–73.

53 X. Dong, L. Q. Ma, Y. Zhu, Y. Li and B. Gu, Mechanistic Investigation of Mercury Sorption by Brazilian Pepper Biochars of Different Pyrolytic Temperatures Based on X-ray Photoelectron Spectroscopy and Flow Calorimetry, *Environ. Sci. Technol.*, 2013, **47**(21), 12156–12164.

54 A. Chagnes and G. Cote, Chemical Degradation of a Mixture of tri-n-Octylamine and 1-Tridecanol in the Presence of Chromium(VI) in Acidic Sulfate Media, *Metals*, 2018, **8**(1), 57.

55 P. L. Smedley and D. G. Kinniburgh, A review of the source, behaviour and distribution of arsenic in natural waters, *Appl. Geochem.*, 2002, **17**(5), 517–568.

56 J. S. Carsella, I. Sánchez-Lombardo, S. J. Bonetti and D. C. Crans, Selenium Speciation in the Fountain Creek Watershed (Colorado, USA) Correlates with Water Hardness, Ca and Mg Levels, *Molecules*, 2017, **22**(5), 708.

57 J. Torres, V. Pintos, L. Gonzatto, S. Domínguez, C. Kremer and E. Kremer, Selenium chemical speciation in natural waters: Protonation and complexation behavior of selenite and selenate in the presence of environmentally relevant cations, *Chem. Geol.*, 2011, **288**(1), 32–38.

58 K. Choi, S. Lee, J. O. Park, J.-A. Park, S.-H. Cho, S. Y. Lee, J. H. Lee and J.-W. Choi, Chromium removal from aqueous solution by a PEI-silica nanocomposite, *Sci. Rep.*, 2018, **8**(1), 1438.

59 N. C. Schroeder, S. D. Radzinski, J. R. Ball, K. R. Ashley, S. L. Cobb, B. Cutrell, J. M. Adams, C. Johnson and G. D. Whitener, Technetium Partitioning for the Hanford Tank Waste Remediation System: anion exchange studies for partitioning technetium from synthetic DSSF and DSS simulants and actual Hanford wastes (101-SY and 103-SY) using Rellex-HPQ resin, Report LA-UR-95-4440 United States: N. p., [online] 1995, (accessed Jan. 1, 2018), DOI: 10.2172/1400218.

60 W. D. King, Evaluation of SuperLig 639 Ion Exchange Resin for the Removal of Rhenium from Hanford Envelope A Simulant; United States, p 33. International Nuclear Information System [online] 2000, https://inis.iaea.org/search/search.aspx?orig_q=RN:31058389, (accessed Jan. 1, 2019).

61 M. L. Gray, *et al.*, A Method for Radioactive Contaminant Removal from Wastewater, *U.S. Pat.*, Application 62814531, 2019.

62 V. E. Jackson, A. R. Felmy and D. A. Dixon, Prediction of the pKa's of Aqueous Metal Ion +2 Complexes, *J. Phys. Chem. At*, 2015, **119**(12), 2926–2939.

63 U.S. Geological Survey, Water Hardness and Alkalinity, [online] 1975, https://water.usgs.gov/owq/hardness-alkalinity.html, (accesesed 6/20/2019).

64 U.S. Environmental Protection Agency, Health and Ecological Criteria Division, *et al.*, Summary Document from the Health Advisory for Boron Compounds, [online] 2008, (accessed June 9, 2019).

65 D. Yu, R. Du, J.-C. Xiao, S. Xu, C. Rong and S. Liu, Theoretical Study of pKa Values for Trivalent Rare-Earth Metal Cations in Aqueous Solution, *J. Phys. Chem. A*, 2018, **122**(2), 700–707.

66 L. Kostenko, N. Kobylinska, S. Khainakov and S. G. Granda, Magnetite nanoparticles with aminomethylenephosphonic groups: synthesis, characterization and uptake of europium(III) ions from aqueous media, *Microchim. Acta*, 2019, **186**(7), 474.

67 D. L. Ramasamy, E. Repo, V. Srivastava and M. Sillanpää, Chemically immobilized and physically adsorbed PAN/acetylacetone modified mesoporous silica for the recovery of rare earth elements from the waste water-comparative and optimization study, *Water Res.*, 2017, **114**, 264–276.

68 L. Bois, A. Bonhommé, A. Ribes, B. Pais, G. Raffin and F. Tessier, Functionalized silica for heavy metal ions adsorption, *Colloids Surf., A*, 2003, **221**(1), 221–230.

69 H.-T. Fan, J. Li, Z.-C. Li and T. Sun, An ion-imprinted amino-functionalized silica gel sorbent prepared by hydrothermal assisted surface imprinting technique for selective removal of cadmium (II) from aqueous solution, *Appl. Surf. Sci.*, 2012, **258**(8), 3815–3822.

70 Q. Wang, W. C. Wilfong, B. W. Kail, Y. Yu and M. L. Gray, Novel Polyethylenimine–Acrylamide/SiO2 Hybrid Hydrogel Sorbent for Rare-Earth-Element Recycling from Aqueous Sources, *ACS Sustainable Chem. Eng.*, 2017, **5**(11), 10947–10958.

